



Robust Beamforming for X-Band Phased Array Weather Radar

Swaroop Sahoo^{*(1)}, Kumar Vijay Mishra⁽²⁾ and Shaik Sharif⁽³⁾

(1) Indian Institute of Technology Palakkad, Palakkad, India

(2) The University of Iowa, Iowa City, IA 52242 USA

(3) Indian Institute of Technology Madras, Chennai, India

Abstract

Phased array weather radars (PAWRs) are increasingly becoming viable because of their operational advantage in the agile scanning of large precipitation volumes without any mechanical motion and an efficient beam scheduling-and-tracking. Conventional PAWR estimates precipitation profiles through Fourier beamforming. However, this method is not robust to interference, clutter and mismatch in steering vectors. In this work, we offset these disadvantages by using advanced robust and adaptive beamformers in PAWR. The volumetric nature of the precipitation target makes direct application of these techniques to PAWR non-trivial. We validate our methods through data collected from the solid-state low-power X-band PAWR developed at IIT Palakkad.

1 Introduction

Monitoring, prediction, and estimation of severe weather phenomena such as flash floods, tornadoes and microbursts is of critical importance [1]. Traditionally, weather radars employ huge parabolic dish antennas and mechanically scan the precipitation volume [2, 3]. This approach is quite inefficient to track very fast moving storms [4]. Recently, phased array weather radars (PAWRs) have been introduced to bring agility and efficiency in the scanning operations. A phased array radar comprises of several antenna elements, that form a highly directional beam without requiring any mechanical motion, achieves beam-steering electronically by adjusting the relative phase of excitation in its constituent elements [5].

The radar estimates the direction-of-arrival (DoA) along the precipitation profiles by adopting spatial filters called beamformers. Conventional technique is Fourier beamforming which is spatial equivalent of a matched filter. It applies uniform phase shift to steer the beam in a specified direction. This computationally simple method is the most optimal in the presence of white noise. However, its precipitation estimates could be considerably biased because of high sidelobe levels. Recently, adaptive beamforming techniques have been employed in phased-array-based atmospheric and weather radars to mitigate the sidelobes of conventional beamformers [6, 7,

8]. These methods have been previously investigated for point-target surveillance radars in detail [9]. However, their application to volumetric targets such as precipitation remains relatively unexamined.

A few studies [7, 6, 10] discuss improvement in sidelobe levels by applying Capon or minimum variance distortionless response (MVDR) beamformer [11] which is capable in rejecting interfering signals such as clutter from directions other than the direction-of-interest. However, this method requires sufficiently high number of samples to accurately estimation of the sample covariance matrix and is prone to steering vector mismatch. In [8], a minimum-mean-squared-error (MMSE) beamformer is proposed which employs prior information to reduce the required number of pulses in the covariance estimation process. The adaptive beamspace processing suggested in [6] improves upon Capon beamformer by making it robust to steering vector mismatch. However, this method is computationally expensive and not useful for real-time deployment.

The performance of most adaptive beamformers degrades when there is an imprecise knowledge of the steering vector, sample size is small or prior information is unavailable. To mitigate these disadvantages, robust adaptive beamforming (RAB) such as diagonal loading [9, 12] has been proposed in point target radars. Although RAB has not been applied to PAWRs so far, their application in other volumetric target sensors such as wind profilers has been very popular. For example the norm-constrained directionally-constrained minimization-of-power (NC-DCMP) beamformer used in [13, 14, 15] for middle and upper troposphere measurements is similar to the classic diagonal loading beamformer [12] and controls the signal-to-noise ratio degradation. It is dependent on the norm constraints whose values are empirically determined in advance. An optimized version of the NC-DCMP was proposed in [7] to increase signal-to-interference-ratio for enhanced probability of detection. This algorithm evaluates residual clutter and noise powers and is especially useful for weak received signals.

In this paper, we investigate RAB beamformers for PAWR. This method will take into consideration various signal

and hardware imperfections and address the problems using the optimized combination of different beamforming techniques. We verify our methods through experimental data obtained by an X-band PAWR developed in-house at IIT Palakkad. In the next section, we describe the system model and various beamformers.

2 Signal Model

Consider a uniformly spaced phased array antenna that has N elements. Then, for the l th snapshot (or pulse repetition interval), the complex-valued discrete-time received signal $N \times 1$ column vector $\mathbf{x}_l = [x_{l,0}, \dots, x_{l,N-1}]^T$ are given by

$$\mathbf{x}_l = \mathbf{A}\mathbf{s}_l + \mathbf{n}_l, \quad (1)$$

where $\mathbf{s}_l = [s_{l,0}, \dots, s_{l,M-1}]^T$ is the source signal vector of M samples from a given range bin, \mathbf{n}_l is additive spatio-temporal white Gaussian noise, $\mathbf{A} = [\mathbf{a}(\theta_0), \dots, \mathbf{a}(\theta_{M-1})]$ is the $N \times M$ receive steering matrix with the i th column

$$\mathbf{a}(\theta_i) = \begin{bmatrix} 1 \\ e^{-j\frac{2\pi}{\lambda} d \sin \theta_i} \\ \vdots \\ e^{-j\frac{2\pi}{\lambda} d (N-1) \sin \theta_i} \end{bmatrix} \quad (2)$$

where d is the channel inter-element spacing, λ is the operating wavelength of the radar, and $(\cdot)^T$ denotes transpose operation.

The received signals \mathbf{x}_l are combined to form complex estimates $\{y_{l,m}\}_{m=1}^{M-1}$ of the precipitation profile from the direction θ_m as follows

$$y_{l,m} = \mathbf{w}^H(\theta_m)\mathbf{x}_l, \quad (3)$$

where $(\cdot)^H$ is the conjugate transpose and $\mathbf{w}(\theta_m)$, $m = 1, \dots, M$ are carefully selected weight vectors. The goal of the beamforming algorithm is to determine $\mathbf{w}(\theta_m)$.

Once the estimates $\{y_{l,m}\}_{m=1}^{M-1}$ are available for L snapshots, standard moments such as the reflectivity (or power), mean Doppler velocity and spectrum width are computed from the autocovariance of $\{y_{l,m}\}_{m=1}^{M-1}$ through the pulse-pair processing method [16]. We now summarize some of the common beamforming method to determine the weight vector.

Fourier Beamformer: This is equivalent to spatial matched filtering. So, the weight vector is simply a copy of the corresponding steering vector, i.e., $\mathbf{w}_{\text{FR}}(\theta_m) = \mathbf{a}(\theta_m)/N$.

Capon/MVDR Beamformer: This method requires only the knowledge of the desired signal direction of arrival and determines the weight vector by solving the optimization

$$\begin{aligned} & \underset{\mathbf{w}(\theta_m)}{\text{minimize}} \quad \mathbf{w}^H(\theta_m)\mathbf{R}_{xx}(0)\mathbf{w}(\theta_m) \\ & \text{subject to} \quad \mathbf{w}^H(\theta_m)\mathbf{a}(\theta_m) = 1, \end{aligned} \quad (4)$$

where $\mathbf{R}_{xx}(0) = \frac{1}{L} \sum_{l=1}^L \mathbf{x}_l \mathbf{x}_l^H$ is the lag-0 autocorrelation of the received signal. The solution of this problem is [17, 18]

$$\mathbf{w}_{\text{CP}}(\theta_m) = \frac{\mathbf{R}_{xx}^{-1}(0)\mathbf{a}(\theta_m)}{\mathbf{a}^H(\theta_m)\mathbf{R}_{xx}^{-1}(0)\mathbf{a}(\theta_m)} \quad (5)$$

Linearly constrained minimum variance (LCMV): If the unity constraint in (4) is changed to $\mathbf{w}^H(\theta_m)\mathbf{a}(\theta_m) = c(\theta_m)$ where c is the constant gain in the direction θ_m , then the resulting spatial filter is called LCMV with weight vectors

$$\mathbf{w}_{\text{CP}}(\theta_m) = \frac{\mathbf{R}_{xx}^{-1}(0)\mathbf{a}(\theta_m)c(\theta_m)}{\mathbf{a}^H(\theta_m)\mathbf{R}_{xx}^{-1}(0)\mathbf{a}(\theta_m)} \quad (6)$$

Diagonal Loading: Since the beamformers involve inversion of a covariance matrix, the numerical stability of the weight vectors is affected while inverting a matrix with small eigen values. The diagonal loading helps with the stability and reduces the spread in weight amplitudes. In this method, a quadratic inequality constraint of bounding the weight coefficients is added to (4) as follows:

$$\begin{aligned} & \underset{\mathbf{w}(\theta_m)}{\text{minimize}} \quad \mathbf{w}^H(\theta_m)\mathbf{R}_{xx}(0)\mathbf{w}(\theta_m) \\ & \text{subject to} \quad \mathbf{w}^H(\theta_m)\mathbf{a}(\theta_m) = 1 \\ & \quad \quad \quad \mathbf{w}^H(\theta_m)\mathbf{w}(\theta_m) \leq T, \end{aligned} \quad (7)$$

where T is the constant norm constraint. The solution to this problem gives

$$\mathbf{w}_{\text{DL}}(\theta_m) = \frac{(\mathbf{R}_{xx} + \alpha\mathbf{I})^{-1}\mathbf{a}(\theta_m)}{\mathbf{a}^H(\theta_m)(\mathbf{R}_{xx} + \alpha\mathbf{I})^{-1}\mathbf{a}(\theta_m)} \quad (8)$$

where α is the diagonal-loading parameter and \mathbf{I} is an identity matrix. The value of $\alpha = 0$ corresponds to Capon/MVDR beamformer while $\alpha = \infty$ denotes nonadaptive beamforming. The intermediate values of α that minimize the total output power are determined based on a set of constraints such that the signal-to-noise and signal-to-interference ratio degradation is minimum. In this work, we compare these various techniques and apply diagonal loading to an X-band PAWR being designed and developed at IIT Palakkad. In the next section, we present details of this system.

3 Radar Specifications

Weather radars at X-band are now being widely used for rain rate measurements because of their low-cost and small size as well as sensitivity to small raindrops sizes [19, 16]. Further, their deployment on mobile platforms [2] and low-power consumption implies that the radars can be deployed in a network. There are also recent efforts toward building solid-state X-band PAWR to allow transmission of low peak powers without losing the radar range resolution.

IIT Palakkad has an ongoing project on designing a solid-state X-band PAWR. The radar transmitter and

Table 1. X-Band PAWR Specifications

Parameter	Value
Operating frequency	9.6 GHz
Peak power	20 W
Pulse width	0.6 μ s
Polarization	Dual polarization
Receiver dynamic range	> 90 dB
Sensitivity	10 dBZ @ 5 km
Receiver noise figure	<4 dB
Minimum Detectable Signal	<-100 dBm
Antenna type	Microstrip patch array
Antenna 3 dB lobe	< 5° elevation and azimuth
Antenna gain	25 dB

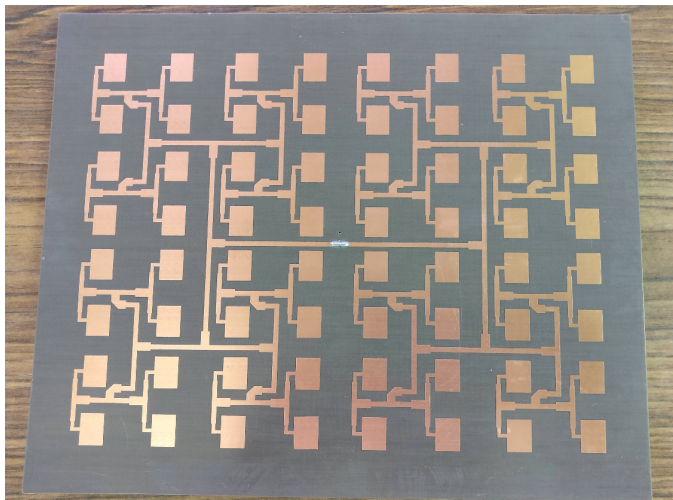


Figure 1. Microstrip patch array antenna designed to operate in the frequency range of 9.6 to 10.6 GHz. Antenna pattern shown in Figure 2 and 3

receiver are based on solid-state components. The waveforms will be transmitted and received both in H- and V-polarizations. The frequency of operation is approximately 9.6 GHz and the peak transmitted power of the signal is approximately 20 W. The radar is still being developed and the transmitter as well as receiver beamwidths will be approximately 5° for any elevation angle. The sensitivity is approximately expected to be 10 dBZ at a range of about 5 km. A volume scan would last less than 1 minute. The receiver is designed to have a dynamic range of 90 dB and a noise figure of less than 4 dB. One of the main requirements of a low-power solid-state X-band radar is an antenna with narrow beamwidth (less than 5°) and low side-lobe (30 dB below the main-lobe) so as to achieve the required resolution at high accuracy [20]. The requirements for low power and small size are being addressed using a microstrip patch array antenna. The antenna is shown in Figure 1 and has physical dimensions of approximately 10 cm on each side. The antenna beam pattern is shown in Figure 2. This antenna has a beamwidth higher than 6° and side lobes are approximately 10 dB below the main lobe [21]. This limitation of the antenna

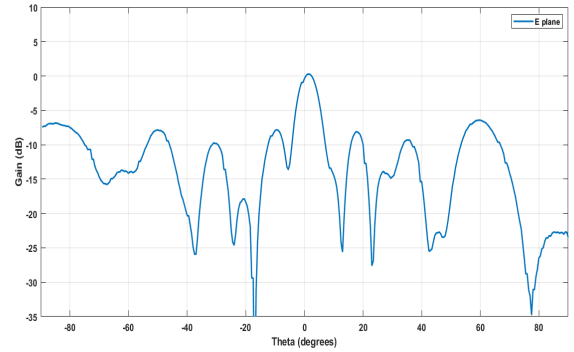


Figure 2. E plane of patch antenna array with a beam width of 8 degrees

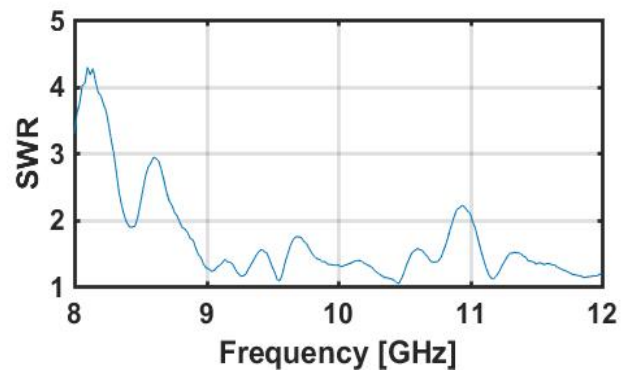


Figure 3. SWR for the patch array antenna

can be mitigated by using phased array that employs robust adaptive beamforming to create a narrow beam and reduce the side lobe levels. The number of antenna elements is 64 and the radar specifications, the antenna voltage-standing-wave-ratio (VSWR) measurements are provided in Table 1, Figure 3, respectively.

This paper reports ongoing efforts to build X-band PAWR and implementation of adaptive beamforming in its signal processor. The radar data analysis will be reported after the deployment of the radar and subsequent field campaigns. The future work involves the development and validation of the radar sub-systems as well as their integration into a single system.

References

- [1] M. Thurai, K. V. Mishra, V. Bringi, and W. F. Krajewski, "Initial results of a new composite-weighted algorithm for dual-polarized X-band rainfall estimation," *Journal of Hydrometeorology*, vol. 18, no. 4, pp. 1081–1100, 2017.
- [2] K. V. Mishra, W. F. Krajewski, R. Goska, D. Ceynar, B.-C. Seo, A. Kruger, J. J. Niemeier, M. B. Galvez, M. Thurai, V. Bringi *et al.*, "Deployment and performance analyses of high-resolution Iowa XPOL radar system during the NASA IFloodS campaign," *Journal of Hydrometeorology*, vol. 17, no. 2, pp. 455–479, 2016.
- [3] K. V. Mishra, A. Kruger, and W. F. Krajewski, "Monitoring cross-channel correlation solar scan measurements using the

- Iowa X-band polarimetric radars,” in *IEEE International Geoscience and Remote Sensing Symposium*, 2013, pp. 1688–1691.
- [4] —, “Compressed sensing applied to weather radar,” in *IEEE International Geoscience and Remote Sensing Symposium*, 2014, pp. 1832–1835.
- [5] K. V. Mishra, I. Kahane, A. Kaufmann, and Y. C. Eldar, “High spatial resolution radar using thinned arrays,” in *IEEE Radar Conference*, 2017, pp. 1119–1124.
- [6] F. Nai, S. M. Torres, and R. D. Palmer, “Adaptive beamspace processing for phased-array weather radars,” *IEEE Transactions on Geoscience and Remote Sensing*, vol. 54, no. 10, pp. 5688–5698, 2016.
- [7] T. Hashimoto, K. Nishimura, M. Tsutsumi, K. Sato, and T. Sato, “A user parameter-free diagonal-loading scheme for clutter rejection on radar wind profilers,” *Journal of Atmospheric and Oceanic Technology*, vol. 54, pp. 1139–1153, 2017.
- [8] E. Yoshikawa, T. Ushio, Z. Kawasaki, S. Yoshida, T. Morimoto, F. Mizutani, and M. Wada, “MMSE beam forming on fast-scanning phased array weather radar,” *IEEE Transactions on Geoscience and remote sensing*, vol. 51, no. 5, pp. 3077–3088, 2013.
- [9] S. A. Vorobyov, “Principles of minimum variance robust adaptive beamforming design,” *Signal Processing*, vol. 93, no. 12, pp. 3264–3277, 2013.
- [10] C. D. Curtis, M. Yeary, and J. L. Lake, “Adaptive nullforming to mitigate ground clutter on the National Weather Radar Testbed Phased Array Radar,” *IEEE Transactions on Geoscience and Remote Sensing*, vol. 54, pp. 1282–1291, 2016.
- [11] J. Capon, “High-resolution frequency-wavenumber spectrum analysis,” in *Proceedings IEEE*, 1969, pp. 1408–1418.
- [12] H. L. Van Trees, *Optimal Array Processing*. New York: Wiley, 2002.
- [13] K. Kamio, K. Nishimura, and T. Sato, “Adaptive sidelobe control for clutter rejection of atmospheric radars,” *Annales Geophysicae*, vol. 22, no. 11, pp. 4005–4012, 2004.
- [14] K. Nishimura, T. Nakamura, T. Sato, and K. Sato, “Adaptive beamforming technique for accurate vertical wind measurements with multichannel MST radar,” *Journal of Atmospheric and Oceanic Technology*, vol. 29, no. 12, pp. 1769–1775, 2012.
- [15] C. D. Curtis, M. Yeary, and J. L. Lake, “Adaptive nullforming to mitigate ground clutter on the National Weather Radar Testbed Phased Array Radar,” *IEEE Transactions on Geoscience and Remote Sensing*, vol. 54, no. 3, pp. 1282–1291, 2016.
- [16] K. V. Mishra, “Frequency diversity wideband digital receiver and signal processor for solid-state dual-polarimetric weather radars,” Master’s thesis, Colorado State University, 2012.
- [17] R. D. Palmer, S. Gopalam, T.-Y. Yu, and S. Fukao, “Coherent radar imaging using capon’s method,” *Radio Science*, vol. 33, pp. 1585–1598, 1998.
- [18] R. D. Palmer, T.-Y. Yu, and P. B. Chilson, “Range imaging using frequency diversity,” *Radio Science*, vol. 34, pp. 1485–1496, 1999.
- [19] K. V. Mishra, V. Chandrasekar, C. Nguyen, and M. Vega, “The signal processor system for the NASA dual-frequency dual-polarized Doppler radar,” in *IEEE International Geoscience and Remote Sensing Symposium*, 2012, pp. 4774–4777.
- [20] M. I. Skolnik, *Introduction to Radar Systems*, 3rd ed. McGraw Hill, 2001.
- [21] S. Sharif and S. Sahoo, “Solid state X-band Doppler radar network for rain rate estimation,” in *IEEE-INAE Workshop on Electromagnetics*, 2018, pp. 1119–1124.